HHS Public Access

Author manuscript

Nat Methods. Author manuscript; available in PMC 2017 October 03.

Published in final edited form as:

Nat Methods. 2017 May ; 14(5): 521–530. doi:10.1038/nmeth.4237.

Generation of mature T cells from human hematopoietic stem/progenitor cells in artificial thymic organoids

Christopher S. Seet[1], **Chongbin He**[2], **Michael T. Bethune**[3], **Suwen Li**[2], **Brent Chick**[2], **Eric H. Gschweng**[4], **Yuhua Zhu**[2], **Kenneth Kim**[2], **Donald B. Kohn**[4,5,6,7], **David Baltimore**[3], **Gay M. Crooks**[2,5,6,7,*], and **Amélie Montel-Hagen**[2,*]

[1]Division of Hematology-Oncology, Department of Medicine, David Geffen School of Medicine (DGSOM), University of California Los Angeles (UCLA)

[2]Department of Pathology & Laboratory Medicine, DGSOM, UCLA

[3]Division of Biology and Biological Engineering, California Institute of Technology, Pasadena

[4]Department of Microbiology, Immunology and Molecular Genetics, DGSOM, UCLA

[5]Division of Pediatric Hematology-Oncology, Department of Pediatrics, DGSOM, UCLA

[6]Broad Stem Cell Research Center, UCLA

[7]Jonsson Comprehensive Cancer Center, UCLA

Abstract

Studies of human T cell development require robust model systems that recapitulate the full span of thymopoiesis, from hematopoietic stem and progenitor cells (HSPCs) through to mature T cells. Existing *in vitro* models induce T cell commitment from human HSPCs; however, differentiation into mature CD3+TCRab+ single positive (SP) CD8+ or CD4+ cells is limited. We describe here a serum-free, artificial thymic organoid (ATO) system that supports highly efficient and reproducible *in vitro* differentiation and positive selection of conventional human T cells from all sources of HSPCs. ATO-derived T cells exhibited mature naïve phenotypes, a diverse TCR

Corresponding Author Information: Gay M. Crooks, M.B., B.S., 610 Charles E. Young Drive, East, 3014 TLSB, Los Angeles, CA 90095, gcrooks@mednet.ucla.edu, Phone: (310) 206 0205, Fax: (310) 206 0356.

*Gay M. Crooks and Amélie Montel-Hagen are co-senior authors

Accession Codes

TCR sequences from this study are deposited in the NCBI GEO repository (accession number: ###).

Author Contributions

C.S.S and A.M.H. designed and performed experiments, analyzed data, prepared figures, and co-wrote the manuscript. C.H. performed histological experiments and with B.C. assisted with *in vivo* experiments. S.L assisted with ATO analysis and T cell functional assays, and K.K. assisted with ATO cultures. Y.Z. performed human specimen processing and cell line cultures. E.G. and D.B.K. provided critical reagents and conceptual advice, and edited the manuscript. M.B. and D.B. devised the approach for and performed TCR repertoire sequencing analysis and provided critical reagents. G.M.C. and A.M.H. co-directed the project and co-wrote the manuscript.

Data Availability

The data that support the findings of this study are available from the corresponding author upon request.

Competing Financial Interests

Kite Pharma, Inc. is supporting the preclinical research of the ATO system at UCLA with Dr. Gay M. Crooks as principal investigator and holds an exclusive license to certain intellectual property relating to the ATO system.

repertoire, and TCR-dependent function. ATOs initiated with TCR-engineered HSPCs produced T cells with antigen specific cytotoxicity and near complete lack of endogenous TCR Vβ expression, consistent with allelic exclusion of Vβ loci. ATOs provide a robust tool for studying human T cell development and stem cell based approaches to engineered T cell therapies.

Due to the spatiotemporal complexity of T cell development in the thymus, *in vitro* models of T cell differentiation have thus far been unable to fully recapitulate human T cell development. A major advance was the discovery that murine stromal cell lines expressing a Notch ligand could support *in vitro* T cell differentiation from murine or human HSPCs, as in the classic OP9-DL1 co-culture system[1, 2, 3]. In this and similar monolayer systems, human cord blood (CB) HSPCs undergo T lineage commitment and rapid early T cell differentiation to CD7+ pro-T cells, followed by CD4 “immature single positive” (CD4ISP) precursors around day 20, and CD4+CD8+ double positive (DP) precursors around day 30[3]. Despite this, positive selection of T cell precursors with productively rearranged TCRs is impaired in OP9-DL1 co-culture, and consequently few CD3+CD8+ or CD4+ single positive (SP) T cells develop[2, 3, 4, 5]. By Day 60–70 on OP9-DL1, mature CD8SP represent at most 2–4% of cultured cells[5]. Improved maturation has been reported using CD34+ HSPC isolated from the human postnatal thymus[6] a population largely composed of lineage committed pro-T cells[7]. However, T cell maturation on OP9-DL1 is particularly inefficient using mobilized peripheral blood and bone marrow HSPCs, the latter giving approximately 10% of the DP and CD3+TCRαβ+ cell yields seen with CB cultures[8].

We and others have shown that three-dimensional (3D) organoid systems using murine[9, 10, 11] or human[12] primary thymic stroma supports improved positive selection and maturation of human T cells *in vitro.* However, these systems are difficult to use given their dependence on primary thymic tissue, and high experimental variability. We therefore sought to develop a system using off-the-shelf, serum-free components able to support efficient and reproducible differentiation and positive selection of human T cells from HSPCs.

We report here the development of an artificial thymic organoid (ATO) system based on a *DLL1*-transduced stromal cell line and serum-free, off-the-shelf components that supported robust differentiation, positive selection, and maturation of human CD3+TCRαβ+CD8SP and CD4SP T cells from CB, bone marrow, and peripheral blood CD34+ HSPCs. Differentiation was efficient whether initiated with CD34+CD3- HSPCs, HSC, or lymphoid progenitors. T cell differentiation in ATOs followed a phenotypic progression that closely recapitulated human thymopoiesis, and was associated with long-term maintenance of CD34+ T cell progenitors.

Both CD3+CD8SP and CD3+CD4SP mature T cells that developed in ATOs exhibited an antigen naïve phenotype, diverse TCR repertoire, and cytokine production and proliferation in response to antigenic stimuli. ATOs also supported highly efficient differentiation of TCR-engineered, antigen-specific T cells from HSPCs transduced with MHC Class I-restricted TCRs specific for the tumor-associated antigens NY-ESO-1 and MART-1. ATO-derived engineered T cells exhibited a naïve phenotype and *in vitro* and *in vivo* antigen-specific cytotoxicity. Moreover, these cells lacked endogenous TCR Vβ expression,

consistent with induction of allelic exclusion by the transduced TCR during early T cell differentiation, and suggesting a new approach to generating potentially non-alloreactive engineered T cells for adoptive immunotherapy. ATOs thus are a standardized and highly efficient *in vitro* model of human T cell development that is readily amenable to genetic manipulation and may permit new approaches to the study of human T cell development.

Results

Development of an optimized artificial thymic organoid system for *in vitro* human T cell differentiation

Our goal was to develop a robust system that supports *in vitro* differentiation and positive selection of human T cells from HSPCs from multiple sources. Based on studies using FTOCs and reaggregated organoids, we hypothesized that 3D structure plays a critical role in T cell positive selection. To avoid the use of primary thymic tissue, we tested *DLL1*-transduced stromal cell lines for their ability to support human T cell development in 3D organoid cultures. As we and others have observed that the efficiency of T cell differentiation in the OP9-DL1 system is highly variable between different lots of fetal calf serum[13], we furthermore sought to identify serum-free conditions capable of supporting T cell differentiation in organoid cultures. To form organoids, we used a simple compaction reaggregation technique[9, 12, 14], by which stromal cells are aggregated with HSPCs by centrifugation and deployed on a cell culture insert at the air-fluid interface (Fig. 1a). Using this method, we identified the MS5 murine bone marrow stromal cell line[15] transduced with human *DLL1* (MS5-hDLL1, hereafter) as strongly supportive of human T cell differentiation and positive selection (measured by the output of mature CD3+TCRαβ +CD8SP cells) from T cell-depleted CD34+ cord blood (CB) HSPCs. We also identified RPMI 1640 supplemented with B27, a multi-component additive used in neuronal and embryonic stem cell cultures[16], and FLT3L, IL-7, and ascorbic acid[17, 18] (“RB27”, hereafter) as a serum-free medium that supported robust human T cell differentiation in MS5-hDLL1 organoid cultures without lot-to-lot variation.

This optimized artificial thymic organoid (ATO) system induced rapid and efficient T lineage commitment from CB CD34+CD3- HSPCs, as shown by a predominance of CD5+CD7+ T-lineage cells and the appearance of CD4+CD3- immature single positive (CD4ISP) and CD4+CD8+ (DP) T cell precursors by week 2 (Fig. 1b). More mature CD3+TCRαβ+ cells emerged as early as week 4 and increased over time, accounting for ~30% of cells at week 6 (Fig. 1b). Long-term maintenance of CD34+ T cell progenitors was also seen in ATOs, and recapitulated the three phenotypic stages of thymic T cell progenitors: multipotent CD34+CD7-CD1a- early thymic progenitors (ETP), and developmentally downstream CD34+CD7+CD1a- and CD34+CD7+CD1a+ pro-T cells (Fig. 1c)[7, 19]. Pro-T1 and pro-T2 progenitor phenotypes, based on an alternative classification scheme using CD5 and CD7[20], were also readily identified within ATO CD34+ cells (Fig. 1c). Consistent with a T lineage-biased ATO microenvironment, CD19+ B cell frequency was low and decreased over time, and NK and myeloid frequencies remained low throughout (Fig. 1b, d). CD3+TCRαβ+ T cell frequency in ATOs was highly consistent across experiments, and included CD8SP and, to a lesser extent, CD4SP T cells, consistent

with positive selection in ATOs (Fig. 1d). A smaller population of CD3+TCRγδ+ T cells was also consistently seen (Fig. 1d). Histological sections of ATOs demonstrated the formation of dense tissue architecture with abundant lymphoid cells (Supplementary Fig. 1), clusters of which expressed CD3 (Fig. 1e).

Each ATO typically generated ~2×10^6 total cells at 6 weeks (Fig. 1f); however, cell yield per HSPC was inversely related to the number of HSPCs seeded and the ratio of HSPCs to stromal cells (Supplementary Fig. 2a). Frequencies of precursor and mature T cells in ATOs was similar across initial HSPC numbers and ratios (Supplemental Fig. 2b), with the exception of ATOs generated with large numbers of stromal cells (6×10^5 per ATO), which showed impaired T cell maturation. Thus, smaller ATOs (typically 7500 HSPCs and 1.5×10^5 stromal cells at a 1:20 ratio) were used for further experiments, and showed high reproducibility of cell output and T cell differentiation across technical replicates (n=11) and was independent of B27 lot (Supplementary Fig. 3a–d). Of translational relevance, efficient T cell differentiation and cell output was also seen in ATOs cultured with xeno-free B27 (Supplementary Fig. 3e, f) or using irradiated MS5-hDLL1 stromal cells (Supplementary Fig. 3g–j). Recovery of hematopoietic cells generated in ATOs after simple mechanical disruption and filtration resulted in >99% CD45+ hematopoietic cells (Supplementary Fig. 3k).

When compared directly to the OP9-DL1 monolayer culture system, ATOs revealed a similar efficiency of T lineage commitment (%CD7+CD5+ cells) but markedly superior generation of both DP and CD3+TCRαβ+ T cells at 4 and 6 weeks (Fig. 2a–d and Supplementary Fig. 4). Improved positive selection was particularly evident in the prevalence of mature CD3+TCRαβ+CD8SP T cells in ATOs but not OP9-DL1 monolayers (Fig. 2b,c,d and Supplementary Fig. 4). Cross-over experiments testing the impact of culture variables revealed that optimal positive selection and T cell maturation required all three components of the ATO system: 3D structure, MS5-hDLL1 stromal cells, and RB27 medium, as neither monolayer cultures using ATO components, nor OP9-DL1 cells in 3D organoids supported T cell development (Supplementary Fig. 5). The parental MS5 cell line lacking *DLL1* expression did not support T cell development in either monolayer or 3D cultures, consistent with a requirement for Notch signaling (Supplementary Fig. 5a).

Recapitulation of thymopoiesis and naïve T cell development in ATOs

T cell differentiation in ATOs was next compared to that in the postnatal human thymus. Week 12 CB ATOs showed a similar frequency of CD34+ pro-T cells and T-lineage committed (CD5+CD7+) cells to the thymus (Fig. 3a). As in the thymus, most CD3+ T cells in ATOs were TCRαβ+ (Fig. 3a). Mature CD3+TCRαβ+ CD8SP and CD4SP T cells increased in frequency in ATOs between weeks 6–12 (Fig. 3b and Supplementary Fig. 6a), and exhibited a reversed CD4:CD8 ratio compared to the thymus.

As in the thymus, ATO-derived CD3+TCRαβ+CD8SP and CD3+TCRαβ+CD4SP T cells transited from a DP-like “immature naïve” (CD45RA-CD45RO+CD27+CCR7-CD1A^{hi}) to a “mature naïve” (CD45RA+CD45RO-CD27+CCR7+CD1a^{lo}) phenotype[21, 22] (Fig. 3c and Supplementary Fig. 6a–c). Both immature and mature naïve T cell subsets co-expressed CD62L and CD28, with subset co-expression of CD127 and CD31, the latter associated with

recent thymic emigrant T cells in the blood[23] (Supplementary Fig. 6b–c). The activation marker CD25 was not expressed on ATO-derived CD8SP T cells, but was observed on a subset of CD4SP T cells (Supplementary Fig. 6b–c). Taken together, these data show remarkable fidelity of T cell differentiation in ATOs compared to the human thymus, culminating in the emergence of naïve T cells phenotypically similar to those in the thymus and blood[24, 25].

Given the absence of thymic epithelial cells and the late emergence and relatively low frequencies of mature CD4SP T cells, we postulated that MHC class II mediated positive selection may rely on the development of rare dendritic cells in ATOs. Indeed, HLA-DR+ cells were present in ATOs at low frequencies, and included monocytes, B cells, and plasmacytoid, CLEC9A+, and CD1c+ dendritic cells (Supplementary Fig. 6d), all of which were also present in the thymus, in agreement with previous reports[26, 27] (Supplementary Fig. 6e).

T cell differentiation from multiple HSPC sources and subsets

In addition to CB, efficient T cell differentiation in ATOs was seen from clinically relevant HSPC sources, i.e. adult bone marrow (BM), G-CSF mobilized peripheral blood (MPB), and non-mobilized peripheral blood (PB) (Fig. 4a–d and Supplementary Fig. 7a,b). Kinetics of T cell differentiation varied between sources (Fig. 4c), with thymic CD34+ cells predictably showing the fastest differentiation; however, T cell output was similar across all sources (Fig. 4d). Enriched hematopoietic stem cell (HSC) fractions (lin-CD34+CD38-)[28] from CB, BM, or MPB also demonstrated efficient T cell differentiation in ATOs (Fig. 4e,f and Supplementary Fig. 7c,d).

ATOs also supported T cell differentiation from highly purified lymphoid progenitors isolated from adult BM (Fig. 4g,h). Lymphoid-primed multipotent progenitors (LMPP)[29] and CD24- common lymphoid progenitors[30] (CLP) generated T cells to a greater extent than unfractionated CD34+lin- HSPCs (Fig. 4g, and Supplementary Fig. 7e,f). In contrast, CD24+ CLPs, which possess primarily B and NK cell potential[30, 31] resulted in poor T cell output in ATOs (Fig. 4g,h and Supplementary Fig. 7e). Thus ATOs can serve as a tool for evaluating T lineage potential in human stem and progenitor cell populations.

TCR diversity and function of ATO-derived T cells

Similar to the thymus, *RAG1* and *RAG2* were expressed at the DP stage in ATOs, consistent with TCR gene rearrangement (Supplementary Fig. 8a). Flow cytometric analysis of TCR Vβ frequencies in ATO-derived CD3+TCRαβ+CD8SP (Fig. 5a) and CD3+TCRαβ+CD4SP (Supplementary Fig. 8b) T cells revealed strikingly similar diversities to those of corresponding naïve T cells from human thymi. Physiological TCR diversity was confirmed by deep sequencing of TCR Vα and Vβ CDR3 regions in ATO-derived CD3+TCRαβ +CD8SP T cells compared with both thymic and PB naïve CD8SP T cells (Fig. 5b,c). Importantly, skewed Vα or Vβ usage was not observed in ATO-derived T cells, arguing against the predominance of unconventional T cell lineages or clonally expanded T cells.

CD8SP T cells isolated from ATOs demonstrated polyfunctional production of IFNγ, TNFα and IL-2 in response to PMA/ionomycin (Fig. 5d), and exhibited upregulation of CD25 and

4-1BB and proliferated in response to anti-CD3/CD28 and IL-2 (Fig. 5e,f). CD4SP cells freshly isolated from ATOs produced IFNγ and IL-2 in response to PMA/ionomycin, and proliferated in response to anti-CD3/CD28 and IL-2 (Supplementary Fig. 8c,d,e).

In vitro generation of naïve TCR-engineered T cells in ATOs

We next explored if ATOs can be used for the *in vitro* generation of naïve TCR-engineered T cells. CB CD34+CD3- HSPCs were transduced with a lentiviral vector encoding codon optimized α and β chains of a HLA-A*02:01-restricted TCR specific for the NY-ESO-$1_{157\text{-}165}$ peptide[32]. At 7 weeks, TCR-transduced ATOs showed a similar frequency of CD7+CD5+ T-lineage cells as mock-transduced controls, but markedly increased CD3+TCRαβ+ T cells, the majority of which expressed the transduced TCR detected by tetramer or an antibody against the transduced Vβ13.1 chain (Fig. 6a). The frequency of tetramer+CD3+TCRαβ+CD8SP T cells was similar to that of mock-transduced ATOs, however TCR transduction resulted in accelerated maturation from an immature (CD45RA-CD45RO+CD27-CCR7-CD1a^{hi}) to a mature (CD45RA+CD45RO-CD27+CCR7+CD1a^{lo}) naïve T cell phenotype (Fig. 6a). As antigen-specific T cells with an unconventional CD8αα phenotype have been reported in the OP9-DL1 system[33], we confirmed that tetramer+ T cells from ATOs displayed a conventional CD8αβ phenotype and lacked expression of CD16 or CD56, markers associated with NK cells and innate-like T cells (Fig. 6b).

TCR transduction also significantly enhanced cell yield from ATOs (average ~500 cells per HSPC) (Fig. 6c), the majority of which were tetramer+CD3+CD8SP T cells. Thus, by 7 weeks a single ATO initiated with 7,500 TCR-transduced HSPCs generated on average ~4×10^6 cells, of which approximately 15% (6×10^5) were mature naïve tetramer +CD3+CD8SPCD45RA+CD45RO- antigen specific T cells (Fig. 6a,c).

ATO-derived antigen specific CD8SP T cells exhibited polyfunctional cytokine production (IFNγ, TNFα and IL-2), degranulation as assessed by CD107a membrane mobilization, (Fig. 6d) and proliferation (Fig. 6e) in response to artificial antigen presenting cells (aAPCs) expressing CD80 and a cognate HLA-A*02:01/NY-ESO-1 single chain trimer; but not irrelevant HLA-A*02:01/MART-1 aAPCs or parental K562 cells. Furthermore, these T cells could be expanded with anti-CD3/CD28 beads and IL-2 or IL-7/IL-15 (Fig. 6f). A previous report of TCR-engineered T cells derived using the OP9-DL1 system reported loss of CD8β expression following repeated *in vitro* stimulation[33], and while a subpopulation of ATO-derived tetramer+CD8SP T cells was CD8β-following re-stimulation with anti-CD3/28 beads, the majority of cells maintained a conventional CD8αβ phenotype (Supplementary Fig. 9a).

Flow cytometric analysis of Vβ diversity in ATO-derived TCR-engineered T cells revealed >98% of tetramer+CD3+CD8SP T cells expressed only the transduced Vβ13.1 segment (Fig. 6g and Supplementary Fig. 9b), suggesting that allelic exclusion of both endogenous Vβ loci occurred during differentiation of TCR-engineered T cells in ATOs.

To test if these findings could be extended beyond the NY-ESO-1 TCR, we generated ATOs using CB HSPCs transduced with an HLA-A*02:01-restricted TCR specific for MART-1[34]. Tetramer+CD3+CD8SP cells isolated from these ATOs demonstrated a naïve T cell

phenotype (Supplemental Fig. 9c) and upregulated IFNγ and mobilized CD107a in response to MART-1 but not NY-ESO-1 aAPCs (Supplemental Fig. 9d).

We next tested antigen-specific cytotoxicity of ATO-derived TCR-engineered T cells. Purified NY-ESO-1-specific CD8SP T cells isolated from TCR-transduced ATOs and activated for 36 hours potently induced apoptosis in cell lines expressing cognate pMHC (either K562 cells transduced with an HLA-A*02:01/NY-ESO-1 SCT; or the HLA-A*02:01+ U266 multiple myeloma cell line which endogenously expresses NY-ESO-1), but showed little activity against parental K562 cells or K562 cells expressing an irrelevant HLA-A*02:01/MART-1 SCT (Fig. 6h and Supplementary Fig. 9e). Consistent with their naïve state, prior activation of ATO-derived antigen-specific T cells was required for cytotoxicity. Loss of antigen specificity was not observed following prolonged (14 days) *in vitro* expansion, indicating retention of a conventional T cell phenotype (Supplementary Fig. 9f); furthermore, cytotoxicity was similar to that of TCR-transduced PB CD8+ T cells expanded for the same period (Supplementary Fig. 9f). Consistent with these results, ATO-derived TCR-engineered T cells were able to significantly control disease progression in NSG mice subcutaneously engrafted with antigen-expressing K562 tumors (Fig. 6i).

Discussion

We present here an *in vitro* system that efficiently initiates and sustains the normal stages of T cell commitment and differentiation from human HSPCs, culminating in the production of mature, naïve CD3+TCRαβ+CD8SP and CD3+TCRαβ+CD4SP T cells closely resembling naïve T cells from the thymus and blood.

Compared to existing methods of *in vitro* T cell differentiation, ATOs supported unprecedented levels of positive selection of CD3+TCRαβ+ precursors into mature CD8SP and CD4SP T cell pools—a process impaired in monolayer systems[2, 3, 4, 5]. Enhanced positive selection in ATOs was strictly dependent on both 3D structure and the stromal cell line used, as monolayer cultures set up with ATO components resulted in inefficient T cell maturation, as did 3D organoid cultures using OP9-DL1 cells. We have however observed mature T cell development in ATOs using *DLL1*-transduced immortalized human BM stromal cells, and while efficiency is lower than for MS5-hDLL1, this indicates that neither species-specific nor MS5-specific factors underlie T cell positive selection in ATOs. We also predict that other Notch ligands, such as DLL4, should be effective in driving T cell development in ATOs.

A specific role for 3D structure in T cell positive selection is consistent with the reported ability of FTOCs and reaggregated primary thymic stromal organoids to permit T cell maturation, albeit at low efficiencies[10, 11, 12]. 3D interactions may support positive selection by increasing the valence and/or duration of contact between T cell precursors and selective ligands (such as pMHC); facilitating crosstalk between stromal and hematopoietic cells; or exerting developmental signals on T cell precursors through mechanical forces and/or metabolic gradients not otherwise possible in 2D. The formation of thymic-like spatial niches segregating developing T cells from stromal signals and/or Notch ligands during development may be another possible mechanism at play in ATOs. In the absence of thymic

epithelial cells in ATOs, we hypothesize that selective MHC I ligands for CD8SP positive selection are ubiquitously presented by hematopoietic cells within the ATOs, as has been suggested in the OP9-DL1 system[6]; but that CD4SP positive selection occurs via MHC class II presentation by dendritic cells that develop within ATOs, with their rarity possibly underlying the bias toward CD8+ T cell development in this system. The nature of these and other specific mechanisms of T cell selection can now be readily investigated using the ATO system in conjunction with model TCR/antigen systems.

Another major advance of the ATO system over existing methods is the efficient generation of mature T cells from clinically relevant adult HSPC sources such as bone marrow, and resting or G-CSF mobilized peripheral blood [2, 3, 4, 5]. While several studies have shown improved T cell maturation on OP9-DL1 using thymic CD34+ cells, these primarily consist of committed pro-T cells[7] and have little therapeutic utility.

ATOs can be used as a novel tool to generate naïve, antigen specific engineered T cells from human HSPCs. Differentiation of TCR-engineered T cells from HPSCs has been reported using the OP9-DL1 system however, as with non-transduced HSPCs, positive selection and generation of mature CD3+ T cells was impaired (typically representing only 0–2% of cultures), with the highest efficiencies achieved using thymic CD34+ cells[33, 35, 36]. In comparison, ATOs strongly supported the differentiation and positive selection of mature CD3+ TCR-engineered T cells from CB HSPCs, with similar results observed using MPB HSPCs (not shown). In contrast to TCR-transduced PB T cells, that require activation and prolonged expansion, *in vitro* generation of naïve antigen specific T cells may offer distinct therapeutic advantages for adoptive cell therapy based on studies correlating earlier T cell differentiation state with *in vivo* efficacy[24, 37, 38]. Non-transduced and TCR-transduced ATOs showed accumulation of naive CD3+CD8SP T cells over time, with concomitant decrease in DPs, consistent with the absence of T cell egress. Despite this, mature T cells in ATOs retained a naïve phenotype, absence of activation markers, and required activation/priming for effective cytotoxicity. TCR transduction of HSPCs also resulted in near-complete allelic exclusion of endogenous Vβ TCR loci, consistent with findings from *in vivo* studies of TCR-transduced murine and human HSPCs[34, 39, 40]. The expression of potentially alloreactive endogenous TCRs on engineered PB T cells is a major barrier to the development of off-the-shelf adoptive T cell therapies, and current approaches to mitigate donor T cell alloreactivity, such as gene editing[41, 42, 43] or the use of virus-specific T cells[44], require extensive cell manipulation, potentially compromising function. We illustrate here that ATOs can be used to exploit developmental allelic exclusion of endogenous TCR expression as a novel strategy for generating potentially non-alloreactive antigen specific T cells for immunotherapy. ATOs are thus a new tool for the study and development of stem cell based engineered T cell therapies, given the ease of genetically manipulating both hematopoietic and stromal compartments, and the ability to produce naïve, unperturbed antigen specific T cells.

Finally, the ATO system offers technical simplicity, reproducibility, and potential scalability. The use of serum-free medium avoids the marked variability observed in monolayer systems[13], and the ability to maintain ATOs intact for the duration of culture (up to 20 weeks) with simple media changes reduces labor through avoiding the frequent transfer of

cells onto fresh stromal cells required by monolayer systems[2, 3, 13]. The simplicity of the ATO system permits straightforward adoption of the method in laboratories interested in studying human T cell development and engineered T cell therapies.

Online Methods

A Supplementary Protocol to aid users accompanies this article and has been deposited at Protocol Exchange (DOI: ####).

Isolation of human CD34+CD3- HSPCs

Neonatal umbilical cord blood was obtained from discarded cord and placental units from deliveries at UCLA. Bone marrow (BM) was obtained from healthy adult donors (ages 18–51) through discarded material from allogeneic BM donor harvests at UCLA or purchased from AllCells Inc. (Alameda, CA). G-CSF mobilized peripheral blood was obtained from consenting healthy adult donors (ages 44–60) undergoing apheresis for allogeneic stem cell transplant donation at UCLA. Non-mobilized peripheral blood was obtained from healthy adult donors through the UCLA CFAR Virology Core. All tissue samples were obtained under UCLA IRB-approved protocols or exemptions. All samples were enriched for mononuclear cells by Ficoll-Paque (GE Healthcare Life Sciences, Pittsburgh, PA) gradient centrifugation followed by positive selection of CD34+ cells by magnetic cell sorting (MACS) using the CD34 MicroBead Kit UltraPure (Miltenyi, Auburn CA). CD34+ cell enriched fractions were cryopreserved after MACS, unless otherwise noted. Prior to use, cells were thawed and residual T cells depleted by FACS by sorting CD34+CD3- cells, which were immediately seeded into ATOs or transduced as described below. In some experiments, HSCs were enriched by FACS for Lin-CD34+CD38- cells prior to seeding in ATOs. HSPCs used in TCR transduction experiments were from HLA-A*02:01+ CB units. High-resolution HLA-A2 typing was performed by the UCLA Immunogenetics Center using sequence-specific oligonucleotide (SSO) beads.

Isolation of human bone marrow progenitor subsets

CD34+ HSPCs were enriched from fresh BM aspirates, as above, and immediately sorted by FACS for stem/progenitor populations based on positive expression of CD45 and absent expression of lineage markers (CD3, CD14, CD19, CD56, and CD235a; “Lin-“) combined with the following markers: total HSPCs (CD34+), HSC (CD34+CD38-CD45RA-)[28, 45], LMPP (CD34+CD38+CD45RA+CD10-CD62L^{hi})[29], CD24- CLP (CD34+CD38+CD45RA +CD10+CD24-)[30], and CD24+ CLP (CD34+CD38+CD45RA+CD10 CD24+)[30, 31].

Isolation of human thymocytes

Postnatal human thymi were obtained under IRB exemption as discarded waste from patients undergoing cardiac surgery at Children’s Hospital Los Angeles (CHLA). Thymic fragments were finely dissected in RPMI and disrupted by pipetting to release thymocytes into suspension, followed by passage through a 70 μm nylon strainer. Cells were analyzed fresh on the same or following day. Flow cytometry analysis of thymic and ATO-derived T cell progenitors used the following surface phenotypes: Early thymic progenitor (ETP; CD34+CD7-CD1a-), CD1a- pro-T (CD34+CD7+CD1a-), and CD1a+ pro-T

(CD34+CD7+CD1a+)[7]; or CD5- pro-T (pro-T1; CD34+CD7+CD5-) and CD5+ pro-T (pro-T2; CD34+CD7+CD5+)[20]. Thymic and ATO-derived T cells and precursors were defined as CD14-CD56- in combination with the following phenotypes: total T lineage cells (CD7+CD5+), double negative (DN; CD4-CD8-), CD4 immature single positive (CD4ISP; CD5+CD4+CD3-), double positive (DP; CD4+CD8+), CD8SP (CD3+TCRαβ +CD8+CD4-), CD4SP (CD3+TCRαβ+CD8-CD4+), immature naïve (CD45RA-CD45RO+ that were CD8SP or CD4SP), mature naïve (CD45RA+CD45RO- that were CD8SP or CD4SP). Immature and mature naïve phenotypes were confirmed by co-staining for CD1a, CD27, CD28, and CCR7.

Isolation of primary human T cells

Thymic T cells were isolated from thymocytes preparations as described above, and peripheral blood and cord blood CD8+ T cells were isolated from mononuclear cell fractions as described above. CD8+ T cell isolation from all sources was by magnetic bead enrichment for CD8SP T cells using the CD8+ T cell Isolation Kit (Miltenyi). In some experiments, thymic T cells were further purified by FACS to deplete CD4ISP or DP precursors, and PB T cells to isolate naïve T cells (CD45RO-CCR7+).

Cell lines

The MS5 murine stromal cell line[15] was obtained as a gift. To generate MS5-hDLL1, MS5 cells were transduced with a lentiviral vector encoding human *DLL1* and eGFP. The highest 5% GFP-expressing cells were sorted by FACS and passaged in DMEM/10% FCS. Stable expression was confirmed by flow cytometry for GFP expression after several weeks of culture, and *DLL1* expression confirmed by qRT-PCR and DNA sequencing. The OP9-DL1 cell line[1] (expressing murine *Dll1*) was a gift from Dr. Juan Carlos Zúñiga-Pflücker (University of Toronto) and was passaged in MEMα (ThermoFisher Scientific, Grand Island, NY)/20% FBS in 0.1% gelatin-coated flasks. The K562 cell line was obtained from ATCC and maintained in RPMI/10% FCS. K562 aAPCs were generated by co-transduction of K562 cells with lentiviral vectors encoding full-length human CD80 and HLA-A*02:01/B2M/NY-ESO-$1_{157\text{-}165}$ or MART-$1_{26\text{-}35}$ single chain trimers (SCTs; gifts from Dr. David Baltimore, Caltech). K562 target cells were created by transduction with either SCT without CD80. Luciferase K562 target cells were created by sequential transduction of K562 cells with a firefly luciferase lentiviral vector (gift from Dr. Donald Kohn, UCLA) followed by either SCT vector. K562 transductants were FACS sorted prior to use. The U266 multiple myeloma cell line was a gift from Dr. John Chute (UCLA) and maintained in RPMI/10% FCS.

Artificial Thymic Organoid (ATO) cultures

MS5-hDLL1 (or MS5 or OP9-DL1, as noted) cells were harvested by trypsinization and resuspended in serum free ATO culture medium (“RB27”) composed of RPMI 1640 (Corning, Manassas, VA), 4% B27 supplement (ThermoFisher Scientific, Grand Island, NY), 30 μM L-ascorbic acid 2-phosphate sesquimagnesium salt hydrate (Sigma-Aldrich, St. Louis, MO) reconstituted in PBS, 1% penicillin/streptomycin (Gemini Bio-Products, West Sacramento, CA), 1% Glutamax (ThermoFisher Scientific, Grand Island, NY), 5 ng/ml rhFLT3L and 5 ng/ml rhIL-7 (Peprotech, Rocky Hill, NJ). RB27 was made fresh weekly. 4%

XenoFree B27 was substituted for B27 in the indicated experiments. Depending on the experiment, 1.5–6×10^5 MS5-hDLL1 cells were combined with 3×10^2–1×10^5 purified CD34+CD3- cells (or other HSPC populations, as indicated) per ATO in 1.5 ml Eppendorf tubes and centrifuged at 300 *g* for 5 min. at 4°C in a swinging bucket centrifuge. Supernatants were carefully removed and the cell pellet was resuspended by brief vortexing. For each ATO, a 0.4 μm Millicell transwell insert (EMD Millipore, Billerica, MA; Cat. PICM0RG50) was placed in a 6-well plate containing 1 ml RB27 per well. To plate ATOs, inserts were taken out and rested on the edge of plate to drain excess medium. The cell slurry was adjusted to 5 μl per ATO, drawn up in with a 20 μl pipet tip and plated by forming a drop at the end of the pipet tip which was gently deposited onto the cell insert. The cell insert was placed back in the well containing 1 mL RB27. Medium was changed completely every 3–4 days by aspiration from around the cell insert followed by replacement with 1 ml with fresh RB27/cytokines. ATOs were cultured in this fashion for up to 20 weeks. At the indicated times, ATO cells were harvested by adding FACS buffer (PBS/0.5% bovine serum album/2mM EDTA) to each well and briefly disaggregating the ATO by pipetting with a 1 ml “P1000” pipet, followed by passage through a 50 μm nylon strainer. In some experiments, single cell suspensions of MS5-hDLL1 cells were γ-irradiated at the indicated doses prior to use in ATOs.

T cell monolayer co-cultures

OP9-DL1 monolayer cultures were set up as previously described[1, 3, 13]. Briefly, OP9-DL1 cells were seeded into 0.1% gelatin-coated 12 well plates 1–2 days prior to use to achieve 70–80% confluence. Medium was aspirated from monolayers and 1.5×10^4 FACS purified CD34+CD3- HSPCs were plated on stromal monolayers in 2 ml of medium composed of MEMα, 20% FBS, 30 μM L-Ascorbic acid, 5 ng/ml rhFLT3L, and 5 ng/ml rhIL-7. In some experiments, MS5 or MS5-hDLL1 was substituted for OP9-DL1, and RB27 was substituted as the culture medium. Cells were transferred to new stromal cell monolayers every 4–5 days by harvesting cells, filtering through a 50 μm nylon strainer, and replating in fresh medium. When confluent, cells were split into multiple wells containing fresh stromal layers.

Lentiviral vectors and transduction

The full-length coding sequence of human *DLL1* was cloned by RT-PCR from a human universal reference RNA set (Agilent Technologies, Santa Clara, CA) into the third generation lentiviral vector pCCL-c-MNDU3-X-IRES-eGFP[34] (gift from Dr. Donald Kohn, UCLA). Human *CD80* was similarly cloned into pCCL-c-MNDU3. The third generation lentiviral vector encoding the codon optimized α and β (Vb13.1) chains of a TCR specific for HLA-A*02:01/NY-ESO-$1_{157\text{-}165}$ (derived from the 1G4 TCR clone[46]) is previously described[32], and was a gift from Dr. Antoni Ribas (UCLA). The codon-optimized HLA-A*02:01/MART-$1_{26\text{-}35}$ specific TCR (derived from the F5 TCR clone[47]) was a gift from Dr. Donald Kohn (UCLA). Coding sequences for HLA-A*02:01/B2M/ NY-ESO-$1_{157\text{-}165}$ or HLA-A*02:01/B2M/ MART-$1_{26\text{-}35}$ single chain trimers were a gift from Dr. David Baltimore (Caltech), and were sub-cloned into the pCCL-c-MNDU3-X-IRES-mStrawberry lentiviral vector. Packaging and concentration of lentivirus particles was performed as previously described[32]. Briefly, 293T cells (ATCC) were co-transfected with a lentiviral

vector plasmid, pCMV-ΔR8.9, and pCAGGS-VSVG using TransIT 293T (Mirus Bio, Madison, WI) for 17 hours followed by treatment with 20 mM sodium butyrate for 8 hours, followed by generation of cell supernatants in serum-free UltraCulture for 48 hours. Supernatants were concentrated by tangential flow filtration using Amicon Ultra-15 100K filters (EMD Millipore, Billerica, MA) at 4000 x*g* for 40 minutes at 4°C and stored as aliquots at −80C. For HSPC transduction, 1×10^5–1×10^6 FACS-sorted CD34+CD3- HSPCs were plated in 6-well non-treated plates coated with 20 μg/ml Retronectin (Clontech, Mountain View, CA) in 1 ml X-VIVO-15 (Lonza, Basel, Switzerland) supplemented with 50 ng/ml of recombinant human SCF, FLT3L, and TPO, and 10 ng/ml IL-3 (Peprotech, Rocky Hill, NJ) for 12–18h, after which concentrated lentiviral supernatant was to a final concentration of 1–2×10^7 TU/ml. Mock-transduced cells were cultured in identical conditions without addition of vector. Cells were harvested 24 hours post-transduction, washed, and seeded into ATOs. For transduction of peripheral blood T cells, CD8+ T cells from healthy donors were isolated by magnetic negative selection using the CD8+ T cell Isolation Kit (Miltenyi) and activated/expanded in AIM V/5% human AB with anti-CD3/CD28 beads (ThermoFisher Scientific) and 20 ng/ml IL-2 for 4 days prior to transduction, as previously described[32]. Transduced T cells were subsequently expanded in IL-2 (20 ng/ml) prior to use.

Immunohistochemistry

For hematoxylin and eosin (H&E) images, ATOs were embedded in Histogel (ThermoFisher Scientific, Grand Island, NY) and fixed overnight in 10% neutral-buffered formalin (ThermoFisher Scientific, Grand Island, NY). 5 μm sections and H&E staining were performed by the UCLA Translational Pathology Core Laboratory (TPCL). For immunofluorescence imaging, ATOs were isolated by cutting the culture insert around each ATO with a scalpel, followed by embedding the membrane and ATO in Tissue-Tek OCT (VWR Radnor, PA) and freezing on dry ice. 5 μm frozen sections were fixed in 10% neutral-buffered formalin and stained with anti-CD3 (clone UCHT1; Biolegend, San Diego, CA) at a 1:50 dilution overnight at 4°C followed by incubation with AlexaFluor 594-conjugated anti-mouse IgG (H+L) (Jackson ImmunoResearch, West Grove, PA) at room temperature. H&E and immunofluorescence images were acquired on a Zeiss AzioImager M2 with AxioCam MRM and AxioVision software (Zeiss, Jena, Germany).

T cell cytokine assays

Mature CD8SP or CD4SP cells from ATOs were isolated by magnetic negative selection using the CD8+ or CD4+ Isolation Kits (Miltenyi) and sorted by FACS to further deplete CD45RO+ cells (containing immature naïve T cells and CD4ISP precursors). Purified T cell populations were plated in 96-well U-bottom plates in 200 μl AIM V (ThermoFisher Scientific, Grand Island, NY) with 5% human AB serum (Gemini Bio-Products, West Sacramento, CA). PMA/ionomycin/protein transport inhibitor cocktail or control protein transport inhibitor cocktail (eBioscience, San Diego, CA) were added to each well and incubated for 6h. Cells were stained for CD3, CD4, and CD8 (Biolegend, San Diego, CA) and UV455 fixable viability dye (eBioscience, San Diego, CA) prior to fixation and permeabilization with an intracellular staining buffer kit (eBioscience, San Diego, CA) and

intracellular staining with antibodies against IFNγ, TNFα, IL-2, IL-4, or IL-17A (Biolegend, San Diego, CA).

T cell activation and proliferation assays

For CFSE proliferation assays, ATO-derived CD8SP or CD4SP T cells were isolated by negative selection MACS as above (with further FACS purification of CD4SP T cells as described above) and labeled with 5 μM CFSE (Biolegend, San Diego, CA). Labeled cells were incubated with anti-CD3/CD28 beads (ThermoFisher Scientific, Grand Island, NY) in AIM V/5% human AB serum with 20 ng/ml rhIL-2 (Peprotech, Rocky Hill, NJ), co-stained for CD25 or 4-1BB (Biolegend, San Diego, CA) and analyzed by flow cytometry on day 5. In some experiments CFSE was substituted for CellTrace Violet (CTV; ThermoFisher) with labeling per the manufacturer's protocol. For *in vitro* cell expansion assays, 5×10^3–1×10^4 ATO-derived CD8SP or CD4SP T cells isolated as above were plated in 96-well U-bottom plates in 200 μl, and activated/expanded with anti-CD3/28 beads and either 20 ng/mL IL-2 or 5 ng/mL IL-7 and 5 ng/mL IL-15 (Peprotech). Beads were removed on day 4, and fresh medium and cytokines were added every 2–3 days with replating into larger wells as needed. Cells were counted weekly with a hemacytometer. In some experiments, cells were restimulated with fresh anti-CD3/CD28 beads on day 14.

Artificial APC (aAPC) CTL priming assay

1×10^5 total ATO-derived CD8SP T cells were isolated from week 6 TCR-transduced ATOs by MACS, as above, and co-cultured with K562-derived aAPCs expressing CD80 and single chain trimers of either HLA-A*02:01/B2M/NY-ESO-$1_{157\text{-}165}$ or HLA-A*02:01/B2M/MART-$1_{26\text{-}35}$ or parental K562 cells in 96-well U-bottom plates in 200 μl AIM V/5% human AB serum at a 2:1 T cell:aAPC ratio for 6h. CD107a-APC antibody (Biolegend, San Diego, CA) was added to wells at a 1:50 final dilution together with a protein transport inhibitor cocktail (eBioscience, San Diego, CA) for the duration of culture. Cells were then stained for surface markers, fixed, permeabilized, and intracellularly stained for cytokines as described above.

TCR Vβ phenotypic analysis

Total cells from pooled week 7 ATOs or postnatal thymi were stained for CD3, CD4, CD8, and TCRγδ, in conjunction with the IOTest Beta Mark TCR V Kit (Beckman Coulter, Indianapolis, IN). CD3+TCRγδ-CD8+CD4- cells were gated for analysis and Vβ family usage was determined by percent FITC+, PE+, or FITC+PE+ cells, representing 3 different Vβ antibodies per tube. For Vβ analysis of TCR-transduced ATOs, total cells from week 6–7 ATOs were additionally labeled with an APC-conjugated HLA-A*02:01/NY-ESO-$1_{157\text{-}165}$ tetramer (MBL International, Woburn, MA) for 10 minutes prior to surface antibody staining, and cells were gated on CD3+TCRγδ-tetramer+CD8+CD4- for Vβ analysis.

TCR repertoire sequencing

Total RNA was purified from 40,000–200,000 FACS sorted ATO or thymic CD3+TCRαβ+CD8SP, or PB CD3+TCRαβ+CD8+CD45RO-CCR7+ naïve CD8+ T cells using the RNeasy Micro kit (Qiagen) according to manufacturer's instructions. RNA concentration

and quality was determined using the Agilent RNA 6000 Nano chip. A targeted cDNA library comprising rearranged TCR variable genes was prepared by 5′-RACE using the SMARTer PCR cDNA Synthesis kit (Clontech) with modifications as follow. First strand cDNA was prepared from 3.5–500 ng total RNA using the manufacturer's protocol but substituting a poly-dT primer (5′-T30VN-3′). Double-stranded TCRα and TCRβ cDNA libraries were prepared separately by semi-nested PCR using the Advantage 2 PCR kit (Clontech). Initial amplification of TCRα cDNA used 0.5 μL first-strand reaction (= 2.5 μL of 1:5 dilution in TE) with the manufacturer's forward Universal Primer Mix and a pair of reverse primers that bound *TRAC* (5′-GCCACAGCACTGTTGCTCTTGAAGTCC-3′). Semi-nested amplification of TCRα cDNA was conducted with manufacturer′s forward Primer IIA and barcoded reverse primers that bound *TRAC* (5′-X5GGCAGGGTCAGGGTTCTGGAT-3′, where X5 is a 5-nt sample-specific barcode enabling sample pooling prior to deep-sequencing). Amplification of TCRβ cDNA was similar but initial amplification was performed with a reverse primer that bound *TRBC* (5′-CCACCAGCTCAGCTCCACGTG-3′) and semi-nested amplification was conducted with barcoded primers that bound *TRBC* (5′-X5GGGAACACSTTKTTCAGGTCCTC-3′). TCRα and TCRβ cDNA preparations were cleaned up using the DNA Clean and Concentrator-5 kit (Zymo Research). TCRα and TCRβ cDNA preparations from up to ten samples were pooled prior to Illumina adaptor ligation and 2 × 150-bp paired-end sequencing on the MiSeq sequencer (Illumina). TCR rearrangements were identified by aligning reads that included the CDR3 to a custom reference sequence library comprising all human TRAV, TRAJ, TRBV, TRBD, and TRBJ sequences contained in the IMGT database[48]. After de-multiplexing using sample-specific barcodes, reads were aligned to a custom reference database comprising all possible combinations of human *TRAV*, *TRAJ*, *TRBV*, *TRBD*, and *TRBJ* sequences downloaded from the IMGT database[48] using BLAT[49]. Best BLAT hits were identified with the pslCDnaFilter utility of the BLAT suite using '-maxAligns=1 –ignoreIntrons' options and clonotype frequencies were calculated using custom Perl scripts (available upon request).

In vitro cytotoxicity assays

CD8SP T cells were isolated from pooled ATOs as described above and were activated in 96 well round-bottom plated in AIM V/5% human AB serum with anti-CD3/CD28 beads (ThermoFisher Scientific) and 20 ng/ml IL-2 for 36h. For extended expansions, cells were cultured in IL-2 for up to 14 days. For cytotoxicity assays, 2-fold serial dilutions of T cells were plated in 96 well round bottom plates starting at 1×10^5 cells per well in AIM V/5% human AB serum. K562 target cells transduced with HLA-A*02:01/NY-ESO-$1_{157\text{-}165}$ or HLA-A*02:01/MART-$1_{26\text{-}35}$ single chain trimers, or U266 multiple myeloma cells were plated at 5×10^4 cells per well. Apoptotic cell death of target cells was quantified by Annexin V/DAPI staining at 9h. Percent antigen-specific T cells was determined by tetramer staining at the start of assays, and used to retrospectively calculate the effector:target (E:T) ratio of each well. T-cell specific cell death was calculated by subtracting percent Annexin V+ target cells in wells receiving no T cells from wells that received T cells.

In vivo tumor assays

All animal experiments were conducted under a protocol approved by the UCLA Chancellor's Animal Research Committee. 4–6 week old male NOD.Cg-Prkdcscid Il2rgtm1Wjl/SzJ (NSG) mice (Jackson Laboratory, Bar Harbor, Maine) were subcutaneously implanted with 2×10^5 K562 target cells transduced with a HLA-A*02:01/NY-ESO-$1_{157\text{-}165}$ single chain trimer and firefly luciferase (as described above). Mice were imaged for tumor bioluminescence on day 3 by intraperitoneal injection of luciferin. ATO-derived CD8SP T cells were isolated and activated/expanded as above for 14 days. 5.7×10^6 T cells (containing 4.5×10^6 antigen-specific T cells as determined by tetramer staining on the day of injection) were injected via retro-orbital vein on day 3 post tumor implantation. Injection of PBS into control mice was also performed. Tumor bioluminescence was repeated every 3–4 days for at least 21 days, after which mice were sacrificed based on disease burden criteria.

Flow Cytometry and Antibodies

All flow cytometry stains were performed in PBS/0.5% BSA/2 mM EDTA for 30 min on ice. FcX (Biolegend, San Diego, CA) was added to all samples for 5 min prior to antibody staining. For tetramer co-staining, PE or APC-conjugated HLA-A*02:01/NY-ESO-$1_{157\text{-}165}$ or HLA-A*02:01/MART-$1_{26\text{-}35}$ tetramers (MBL International, Woburn, MA) were added to cells at a 1:50 final dilution at room temperature for 10 minutes prior to addition of antibodies for an additional 20 minutes on ice. DAPI was added to all samples prior to analysis. Analysis was performed on an LSRII Fortessa, and FACS on an ARIA or ARIA-H instrument (BD Biosciences, San Jose, CA) at the UCLA Broad Stem Cell Research Center Flow Cytometry Core. For all analyses DAPI+ cells were gated out, and single cells were gated based on FSC-H vs. FSC-W and SSC-H vs. SSC-W. Antibody clones used for surface and intracellular staining were obtained from Biolegend (San Diego, CA): CD1a (HI149), CD3 (UCHT1), CD4 (RPA-T4), CD5 (UCHT2), CD8 (SK1), CD10 (6H6), CD14 (M5E2), CD19 (HIB19), CD24 (ML5), CD25 (BC96), CD27 (O323), CD28 (CD28.2), CD31 (WM59), CD34 (581), CD38 (HIT2), CD45 (HI30), CD45RA (HI100), CD45RO (UCHL1), CD56 (HCD56), CD107a (H4A3), CD127 (A019D5), CD235a (HI264), CCR7 (G043H7), HLA-A2 (BB7.2), interferon γ (4S.B3), IL-2 (MQ1-17H12), IL-4 (MP4-25D2), IL-17A (BL168), TCRαβ (IP26), TCRγδ (B1), TNFα (Mab11), Vβ13.1 (H131), human lineage cocktail (CD3, CD14, CD19, CD20, CD56); and BD Biosciences (San Jose, CA): CD7 (M-T701), and CD62L (DREG-56).

Statistical Analysis

For Fig. 6c and Fig. 6i, statistics were analyzed using a two-tailed unpaired *t* test. Exact *n* values for all experiments are specified in figure legends.

Supplementary Material

Refer to Web version on PubMed Central for supplementary material.

Acknowledgments

We would like to thank Jessica Scholes and Felicia Codrea at the UCLA Broad Stem Cell Research Center (BSCRC) Flow Cytometry Core for assistance with FACS sorting; Rebecca Chan for assistance with specimen

processing; Dr. Chintan Parekh from Children's Hospital Los Angeles for generous assistance with thymus samples; Dr. Mary Sehl (UCLA) for assistance with MPB collection, and Dr. Aaron Cooper (UCLA) for helpful advice and discussion. We thank Dr. Igor Antoshechkin of The Millard and Muriel Jacobs Genetics and Genomics Laboratory at Caltech, who developed the method for and assisted with TCR sequencing analysis. This work was supported by NIH grants R01 AG049753 (G.M.C.), 1R21AI119927 (G.M.C. and A.M.H.), P01 HL073104 (G.M.C. and D.B.K.), and T32HL066992 (C.S.S.); Tower Cancer Research Foundation (C.S.S.); UCLA BSCRC Innovation award (G.M.C. and D.B.K.) and BSCRC Clinical Fellowship (C.S.S.). M.T.B. and D.B. are supported by Prostate Cancer Foundation Challenge Award 15CHAL02 and M.T.B is the recipient of a Jane Coffin Childs Postdoctoral Fellowship. Core services were supported by the UCLA Jonsson Comprehensive Cancer Center Shared facility (TPCL, grant 5P30CA016042), UCLA Immunogenetics Center, UCLA Center for AIDS Research Virology Core Lab and UCLA AIDS Institute (grant 5P30 AI028697), and the Millard and Muriel Jacobs Genetics and Genomics Laboratory at Caltech.

References

1. Schmitt TM, Zúñiga-Pflücker JC. Induction of T Cell Development from Hematopoietic Progenitor Cells by Delta-like-1 In Vitro. Immunity. 2002; 17:749–756. [PubMed: 12479821]
2. De Smedt M, Hoebeke I, Plum J. Human bone marrow CD34+ progenitor cells mature to T cells on OP9-DL1 stromal cell line without thymus microenvironment. Blood Cells Mol Dis. 2004; 33:227–232. [PubMed: 15528136]
3. La Motte-Mohs RN, Herer E, Zuniga-Pflucker JC. Induction of T-cell development from human cord blood hematopoietic stem cells by Delta-like 1 in vitro. Blood. 2005; 105:1431–1439. [PubMed: 15494433]
4. de Pooter R, Zúñiga-Pflücker JC. T-cell potential and development in vitro: the OP9-DL1 approach. Current Opinion in Immunology. 2007; 19:163–168. [PubMed: 17303399]
5. Awong G, Herer E, La Motte-Mohs RN, Zuniga-Pflucker JC. Human CD8 T cells generated in vitro from hematopoietic stem cells are functionally mature. BMC Immunol. 2011; 12:22. [PubMed: 21429219]
6. Van Coppernolle S, et al. Functionally mature CD4 and CD8 TCRalphabeta cells are generated in OP9-DL1 cultures from human CD34+ hematopoietic cells. Journal of immunology (Baltimore, Md : 1950). 2009; 183:4859–4870.
7. Hao QL, et al. Human intrathymic lineage commitment is marked by differential CD7 expression: identification of CD7- lympho-myeloid thymic progenitors. Blood. 2008; 111:1318–1326. [PubMed: 17959857]
8. De Smedt M, et al. T-lymphoid differentiation potential measured in vitro is higher in CD34+CD38-/lo hematopoietic stem cells from umbilical cord blood than from bone marrow and is an intrinsic property of the cells. Haematologica. 2011; 96:646. [PubMed: 21330325]
9. Anderson G, Jenkinson EJ, Moore NC, Owen JJT. MHC class II-positive epithelium and mesenchyme cells are both required for T-cell development in the thymus. Nature. 1993; 362:70–73. [PubMed: 8446171]
10. Plum J, De Smedt M, Defresne M, Leclercq G, Vandekerckhove B. Human CD34+ fetal liver stem cells differentiate to T cells in a mouse thymic microenvironment. Blood. 1994; 84:1587–1593. [PubMed: 7520780]
11. Poznansky MC, et al. Efficient generation of human T cells from a tissue-engineered thymic organoid. Nat Biotech. 2000; 18:729–734.
12. Chung B, et al. Engineering the human thymic microenvironment to support thymopoiesis in vivo. Stem Cells. 2014; 32:2386–2396. [PubMed: 24801626]
13. Awong, G., Motte-Mohs, RNL., Zúñiga-Pflücker, JC. In Vitro Human T Cell Development Directed by Notch–Ligand Interactions. In: Bunting, KD., editor. Hematopoietic Stem Cell Protocols. Humana Press; Totowa, NJ: 2008. p. 135-142.
14. Sheridan JM, Taoudi S, Medvinsky A, Blackburn CC. A novel method for the generation of reaggregated organotypic cultures that permits juxtaposition of defined cell populations. genesis. 2009; 47:346–351. [PubMed: 19370754]
15. Itoh K, et al. Reproducible establishment of hemopoietic supportive stromal cell lines from murine bone marrow. Experimental hematology. 1989; 17:145–153. [PubMed: 2783573]

16. Brewer GJ, Torricelli JR, Evege EK, Price PJ. Optimized survival of hippocampal neurons in B27-supplemented Neurobasal, a new serum-free medium combination. Journal of neuroscience research. 1993; 35:567–576. [PubMed: 8377226]
17. Huijskens MJAJ, et al. Technical Advance: Ascorbic acid induces development of double-positive T cells from human hematopoietic stem cells in the absence of stromal cells. Journal of Leukocyte Biology. 2014; 96:1165–1175. [PubMed: 25157026]
18. Manning J, et al. Vitamin C promotes maturation of T-cells. Antioxidants & redox signaling. 2013; 19:2054–2067. [PubMed: 23249337]
19. Casero D, et al. Long non-coding RNA profiling of human lymphoid progenitor cells reveals transcriptional divergence of B cell and T cell lineages. Nature immunology. 2015; 16:1282–1291. [PubMed: 26502406]
20. Awong G, et al. Characterization in vitro and engraftment potential in vivo of human progenitor T cells generated from hematopoietic stem cells. Blood. 2009; 114:972–982. [PubMed: 19491395]
21. Vanhecke D, Leclercq G, Plum J, Vandekerckhove B. Characterization of distinct stages during the differentiation of human CD69+CD3+ thymocytes and identification of thymic emigrants. Journal of immunology (Baltimore, Md : 1950). 1995; 155:1862–1872.
22. Res P, Blom B, Hori T, Weijer K, Spits H. Downregulation of CD1 marks acquisition of functional maturation of human thymocytes and defines a control point in late stages of human T cell development. The Journal of experimental medicine. 1997; 185:141–151. [PubMed: 8996250]
23. Kimmig S, et al. Two subsets of naive T helper cells with distinct T cell receptor excision circle content in human adult peripheral blood. The Journal of experimental medicine. 2002; 195:789–794. [PubMed: 11901204]
24. Hinrichs CS, et al. Adoptively transferred effector cells derived from naive rather than central memory CD8+ T cells mediate superior antitumor immunity. Proceedings of the National Academy of Sciences of the United States of America. 2009; 106:17469–17474. [PubMed: 19805141]
25. Restifo NP, Dudley ME, Rosenberg SA. Adoptive immunotherapy for cancer: harnessing the T cell response. Nat Rev Immunol. 2012; 12:269–281. [PubMed: 22437939]
26. Gurka S, Dirks S, Photiadis J, Kroczek RA. Expression analysis of surface molecules on human thymic dendritic cells with the 10th HLDA Workshop antibody panel. Clinical & Translational Immunology. 2015; 4:e47. [PubMed: 26682055]
27. Martinez VG, et al. A discrete population of IFN [lambda]-expressing BDCA3hi dendritic cells is present in human thymus. Immunol Cell Biol. 2015; 93:673–678. [PubMed: 25753268]
28. Hao QL, Shah AJ, Thiemann FT, Smogorzewska EM, Crooks GM. A functional comparison of CD34 + CD38- cells in cord blood and bone marrow. Blood. 1995; 86:3745–3753. [PubMed: 7579341]
29. Kohn LA, et al. Lymphoid priming in human bone marrow begins before expression of CD10 with upregulation of L-selectin. Nature immunology. 2012; 13:963–971. [PubMed: 22941246]
30. Six EM, et al. A human postnatal lymphoid progenitor capable of circulating and seeding the thymus. The Journal of experimental medicine. 2007; 204:3085–3093. [PubMed: 18070935]
31. Galy A, Travis M, Cen D, Chen B. Human T, B, natural killer, and dendritic cells arise from a common bone marrow progenitor cell subset. Immunity. 1995; 3:459–473. [PubMed: 7584137]
32. Gschweng EH, et al. HSV-sr39TK positron emission tomography and suicide gene elimination of human hematopoietic stem cells and their progeny in humanized mice. Cancer research. 2014; 74:5173–5183. [PubMed: 25038231]
33. Snauwaert S, et al. In vitro generation of mature, naive antigen-specific CD8(+) T cells with a single T-cell receptor by agonist selection. Leukemia. 2014; 28:830–841. [PubMed: 24091848]
34. Giannoni F, et al. Allelic exclusion and peripheral reconstitution by TCR transgenic T cells arising from transduced human hematopoietic stem/progenitor cells. Mol Ther. 2013; 21:1044–1054. [PubMed: 23380815]
35. Zhao Y, et al. Extrathymic generation of tumor-specific T cells from genetically engineered human hematopoietic stem cells via Notch signaling. Cancer research. 2007; 67:2425–2429. [PubMed: 17363559]

36. van Lent AU, et al. Functional human antigen-specific T cells produced in vitro using retroviral T cell receptor transfer into hematopoietic progenitors. Journal of immunology (Baltimore, Md : 1950). 2007; 179:4959–4968.
37. Gattinoni L, et al. Acquisition of full effector function in vitro paradoxically impairs the in vivo antitumor efficacy of adoptively transferred CD8+ T cells. The Journal of clinical investigation. 2005; 115:1616–1626. [PubMed: 15931392]
38. Hinrichs CS, Rosenberg SA. Exploiting the curative potential of adoptive T-cell therapy for cancer. Immunological Reviews. 2014; 257:56–71. [PubMed: 24329789]
39. Vatakis DN, et al. Introduction of exogenous T-cell receptors into human hematopoietic progenitors results in exclusion of endogenous T-cell receptor expression. Mol Ther. 2013; 21:1055–1063. [PubMed: 23481324]
40. Starck L, Popp K, Pircher H, Uckert W. Immunotherapy with TCR-redirected T cells: comparison of TCR-transduced and TCR-engineered hematopoietic stem cell-derived T cells. Journal of immunology (Baltimore, Md : 1950). 2014; 192:206–213.
41. Torikai H, et al. A foundation for universal T-cell based immunotherapy: T cells engineered to express a CD19-specific chimeric-antigen-receptor and eliminate expression of endogenous TCR. Blood. 2012; 119:5697–5705. [PubMed: 22535661]
42. Berdien B, Mock U, Atanackovic D, Fehse B. TALEN-mediated editing of endogenous T-cell receptors facilitates efficient reprogramming of T lymphocytes by lentiviral gene transfer. Gene therapy. 2014; 21:539–548. [PubMed: 24670996]
43. Poirot L, et al. Multiplex Genome-Edited T-cell Manufacturing Platform for “Off-the-Shelf” Adoptive T-cell Immunotherapies. Cancer research. 2015; 75:3853–3864. [PubMed: 26183927]
44. Themeli M, Riviere I, Sadelain M. New cell sources for T cell engineering and adoptive immunotherapy. Cell stem cell. 2015; 16:357–366. [PubMed: 25842976]
45. Majeti R, Park CY, Weissman IL. Identification of a hierarchy of multipotent hematopoietic progenitors in human cord blood. Cell stem cell. 2007; 1:635–645. [PubMed: 18371405]
46. Robbins PF, et al. Single and dual amino acid substitutions in TCR CDRs can enhance antigen-specific T cell functions. Journal of immunology (Baltimore, Md : 1950). 2008; 180:6116–6131.
47. Johnson LA, et al. Gene Transfer of Tumor-Reactive TCR Confers Both High Avidity and Tumor Reactivity to Nonreactive Peripheral Blood Mononuclear Cells and Tumor-Infiltrating Lymphocytes. The Journal of Immunology. 2006; 177:6548–6559. [PubMed: 17056587]
48. Giudicelli V, Chaume D, Lefranc MP. IMGT/GENE-DB: a comprehensive database for human and mouse immunoglobulin and T cell receptor genes. Nucleic Acids Research. 2005; 33:D256–D261. [PubMed: 15608191]
49. Kent WJ. BLAT—The BLAST-Like Alignment Tool. Genome Research. 2002; 12:656–664. [PubMed: 11932250]

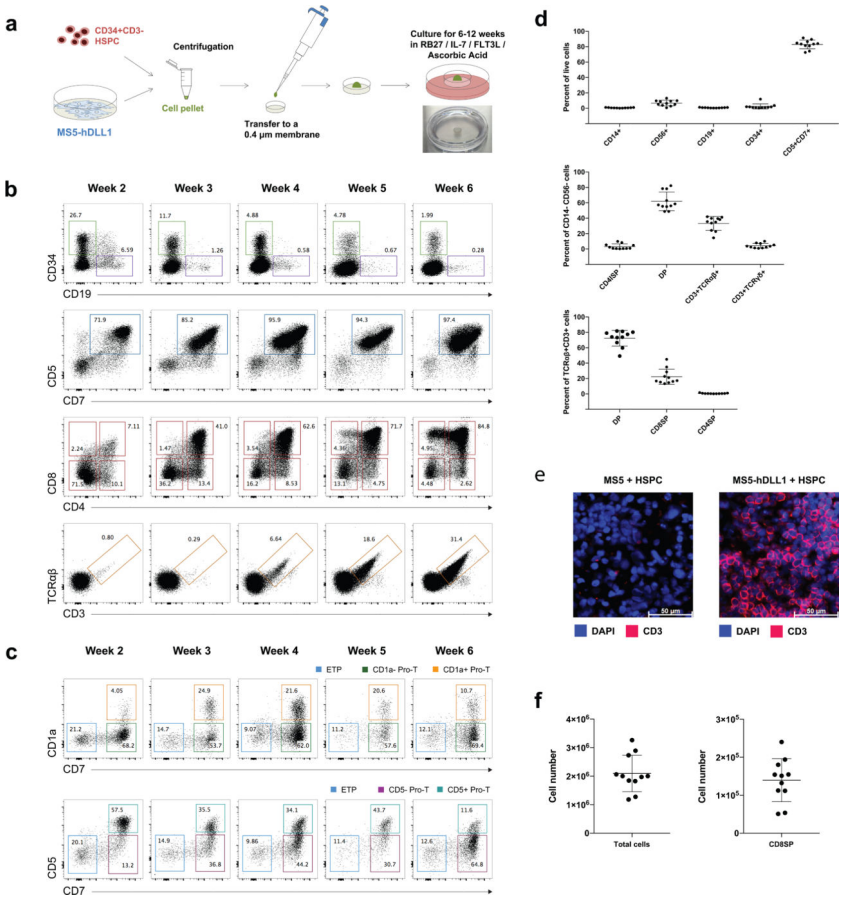

Figure 1. Efficiency and reproducibility of human T cell development in the ATO system

(a) Schematic of the ATO model. Inset: appearance of a typical ATO attached to cell culture insert at 6 weeks (shown after removal from culture well). **(b)** Kinetics of T cell differentiation from CB CD34+CD3- HSPCs at the indicated weeks, gated on CD14-CD56- cells to exclude monocytes and NK cells respectively. **(c)** Maintenance of early CD34+ thymic T cell progenitor phenotypes in ATOs based on two classification schemes, both gated on CD34+ cells as shown in (b). **(d)** Frequencies of cell types in ATOs at 6 weeks. Top panel: frequencies of monocytes (CD14+), NK cells (CD56+), B cells (CD19+), HSPCs (CD34+), or T lineage cell (CD7+CD5+) (gated on total live cells). Middle panel: T cell precursor and TCR+ T cell frequencies (gated on CD14-CD56- cells). Bottom panel: frequency of DP and mature CD8 and CD4 single positive (SP) T cells (gated on CD3+TCRαβ+ cells). **(e)** CD3 expression by **i**mmunofluorescence analysis in week 4 organoids generated with CB HSPCs and MS-5 cells (left) or MS5-hDLL1 cells (i.e. ATO) (right). **(f)** Numbers of total live cells and CD3+TCRαβ+CD8SP T cells generated per ATO at week 6 from 7.5–22.5 $\times 10^3$ CB HSPCs per ATO. Data are shown for 11 independent experiments (error bars indicate standard deviation).

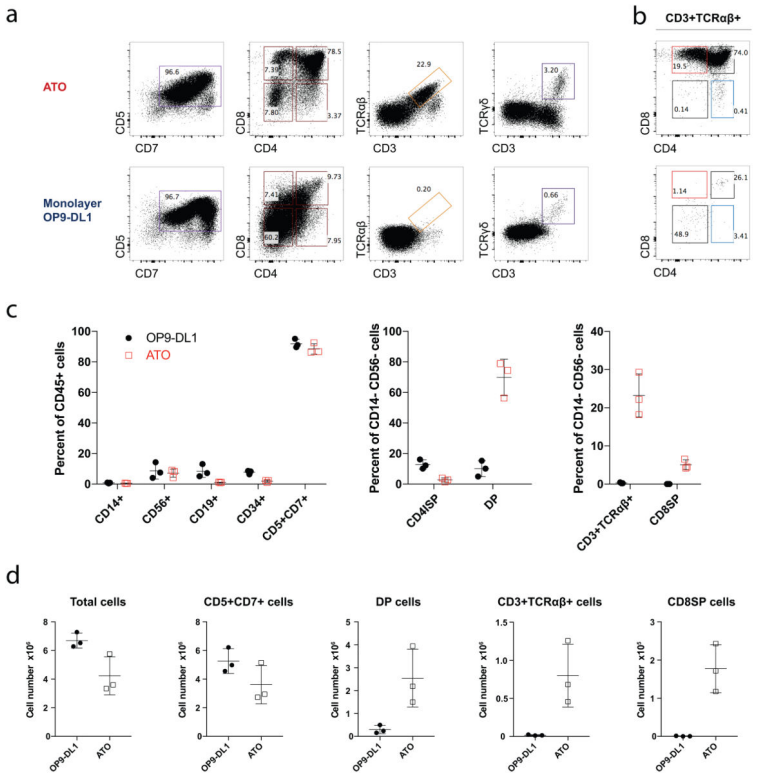

Figure 2. Enhanced positive selection in the ATO system compared to OP9-DL1 monolayers

CD34+CD3- HSPCs from the same cord blood donor were used to initiate ATOs or standard OP9-DL1 monolayer cultures (containing 20% FBS) in parallel, and analyzed by flow cytometry and cell counting. Shown are data from 6 week cultures. **(a,b)** Representative flow cytometry profiles of cells gated on **(a)** total CD14-CD56- cells and (**b**) CD3+TCRαβ+ cells. **(c,d)** Summary of data from three different cord blood donors used to initiate parallel ATO and OP9-DL1 cultures. **(c)** Frequencies of monocytes (CD14+), NK cells (CD56+), B cells (CD19+), HSPCs (CD34+), or T lineage cells (CD7+CD5+) (gated on total CD45+ cells); CD4ISP and DP T cell precursors, and CD3+TCRαβ+ and CD3+TCRαβ+CD8SP mature T cells (gated on CD14-CD56- cells) in OP9-DL1 monolayer co-cultures versus ATOs at 6 weeks. Error bars represent the SD of three independent experiments. **(d)** Absolute numbers of T cell subsets at week 6 in OP9-DL1 co-cultures versus ATOs using the frequency data shown in (c). OP9-DL1 cultures were each initiated with 1.5×10^4 CD34+CD3- CB HSPCs cells, and ATOs were each initiated with 7.5×10^3 HSPCs from the same cord blood unit with technical duplicate ATOs harvested and pooled at 6 weeks for comparison of cell counts. Bars represent the mean and SD of three independent experiments.

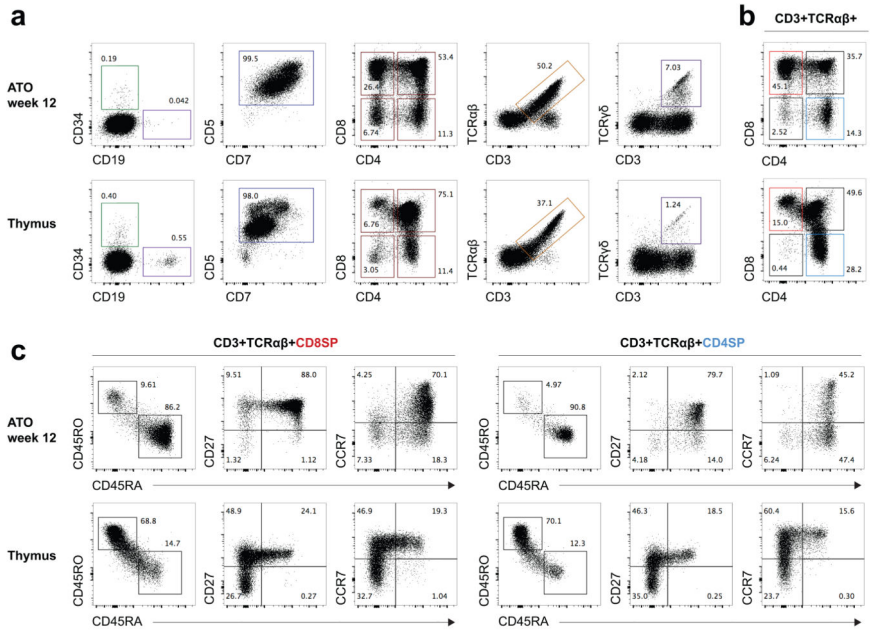

Figure 3. Recapitulation of thymopoiesis and naïve T cell development in ATOs

Comparison of T cell differentiation in CB ATOs at 12 weeks and human postnatal thymocytes, gated on **(a)** total CD14-CD56- and (**b**) CD3+TCRαβ+ cells. **(c)** Generation of immature (CD45RA-CD45RO+) and mature (CD45RA+CD45RO-) naïve T cells in ATOs or thymus (gated on CD3+TCRαβ+ cells, with CD8SP or CD4SP subgates indicated). Data are representative of three independent experiments.

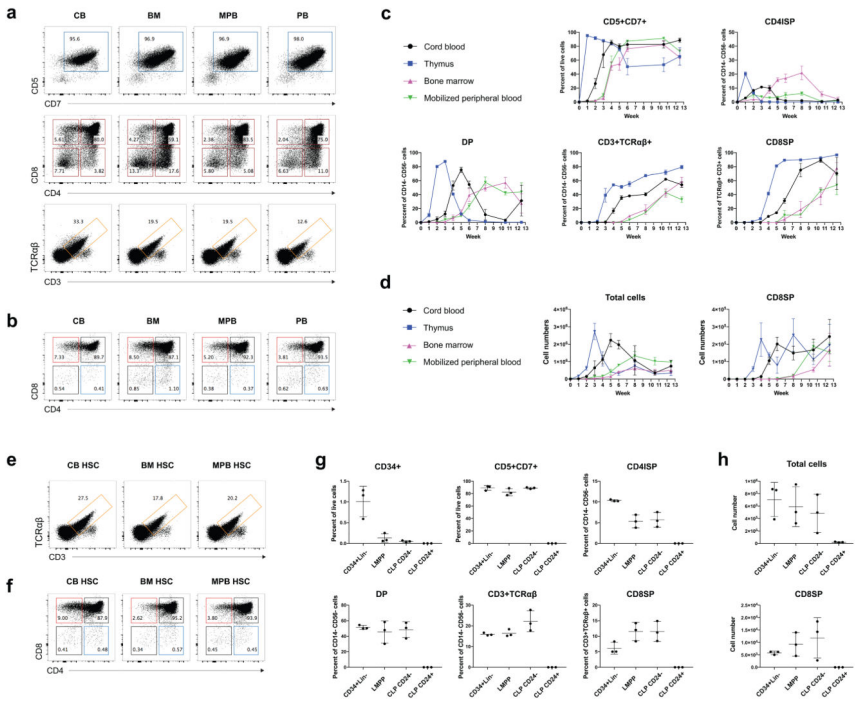

Figure 4. Generation of T cells from multiple HSPC sources and subsets

Efficient T cell development in week 6 ATOs initiated with CD34+CD3- HSPCs from human cord blood (CB), adult bone marrow (BM), G-CSF mobilized peripheral blood (MPB), or non-mobilized peripheral blood (PB). Gated on **(a)** total CD14-CD56- cells, and **(b)** CD3+TCRαβ+ T cells. **(c)** T cell differentiation kinetics over 12 weeks in ATOs generated from 7500 CD34+CD3- cells isolated from CB, neonatal thymi, BM, or MPB. Mean and SD of T cell precursor and mature T cells frequencies are shown from three technical replicates per tissue. Data are representative of two different experiments. **(d)** Numbers of total cells and CD3+TCRαβ+CD8SP T cells from ATO experiments shown in (c). **(e)** T cell differentiation from hematopoietic stem cell (HSC)-enriched (Lin-CD34+CD38-) fractions from CB, BM, and MPB in week 6 ATOs, gated on CD14-CD56- cells and **(f)** CD3+TCRαβ+ T cells. Data are representative of independent experiments (CB n=3, BM n=2, and MPB n=1). **(g)** T cell differentiation potential of adult BM total HSPCs (CD34+lin-) and purified progenitor (LMPP and CLP) subsets in ATOs at week 6; frequencies of CD34+ HSPCs, total T lineage cells (CD5+CD7+) and different T cell subsets are shown. **(h)** Numbers of total cells and CD3+TCRαβ+CD8SP T cells from ATOs shown in (g). Mean and SD of technical triplicates are shown for (g) and (h), and data are representative of three independent experiments.

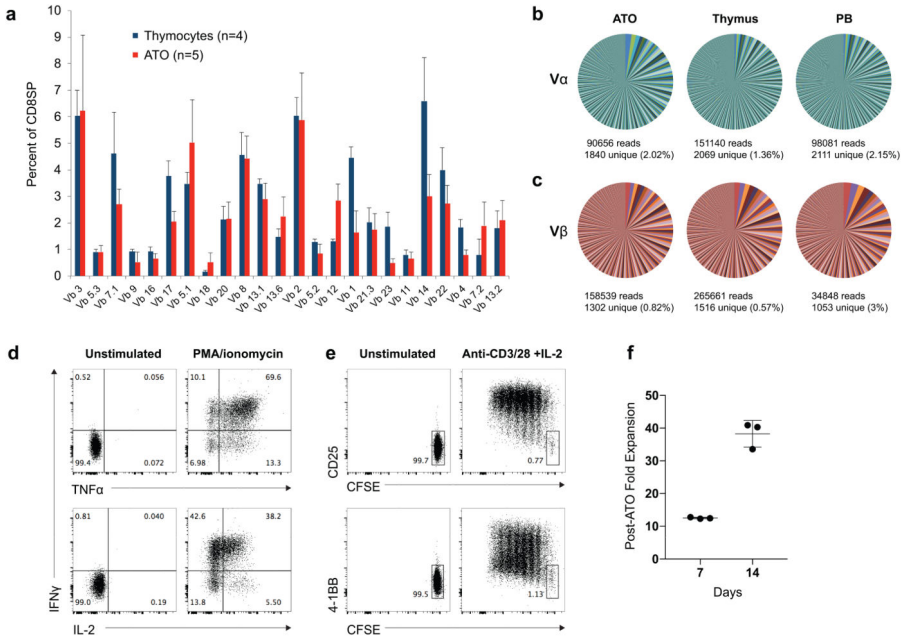

Figure 5. TCR diversity and function of ATO-derived T cells

(a) Generation of TCR diversity in CD3+TCRαβ+CD8SP T cells from week 7 ATOs (n=5) or human thymi (n=4), as shown by flow cytometric analysis of the frequency of TCR Vβ family expression. **(b)** TCR clonotype diversity in CD3+TCRαβ+CD8SP T cells from ATOs, thymus, and peripheral blood (PB) naïve T cells by deep sequencing of TCR Vα and **(c)** TCR Vβ CDR3 regions. Frequency of individual clonotypes is shown. Data are representative of three independent experiments. **(d)** Polyfunctional cytokine production by ATO-derived CD3+TCRαβ+CD8SP T cells treated with PMA/ionomycin for 6h. Data are representative of three individual experiments. **(e)** Proliferation (CFSE dilution) and activation (upregulation of CD25 and 4-1BB) of ATO-derived CD3+TCRαβ+CD8SP cells after 5 days in response to anti-CD3/CD28 and IL-2. Data are representative of two individual experiments. **(f)** Post-ATO expansion of ATO-derived CD3+TCRαβ+CD8SP T cells relative to starting cell number in response to anti-CD3/CD28 and IL-2 after 7 and 14 days. Mean and SD of technical triplicates are shown, and data are representative of three independent experiments.

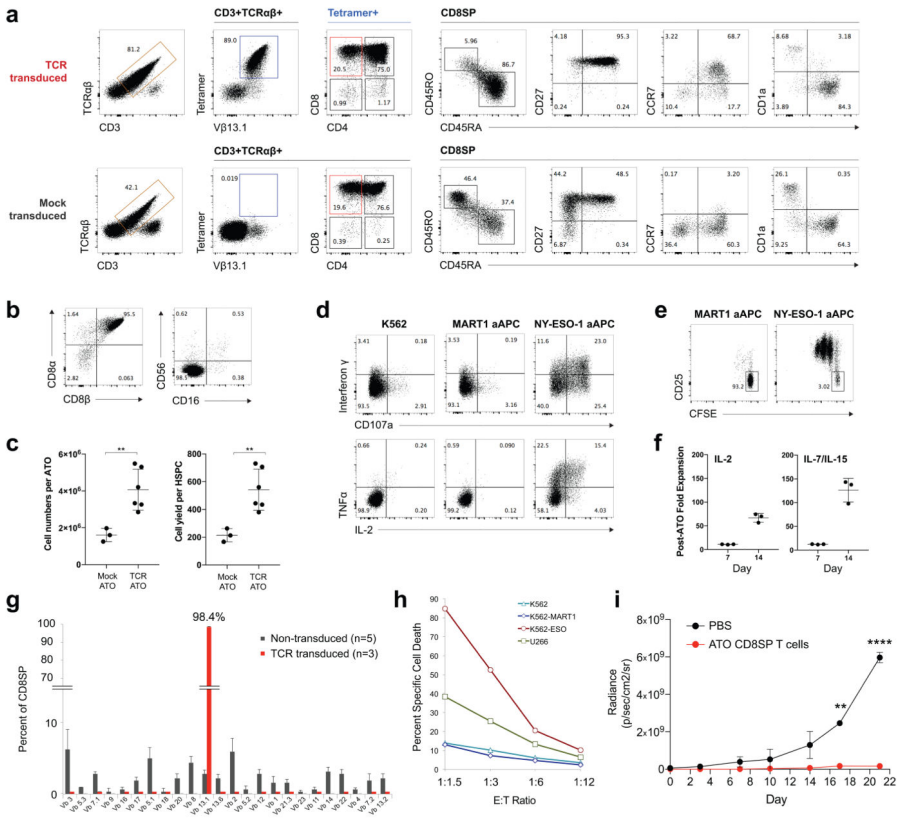

Figure 6. Differentiation and allelic exclusion of TCR-engineered T cells in ATOs

(a) Efficient generation of HLA-A*0201/NY-ESO-$1_{157\text{-}165}$ specific TCR-engineered T cells in week 7 ATOs initiated with TCR-transduced (top row) versus mock-transduced (bottom row) CB CD34+CD3- HSPCs. Cells are gated on CD14-CD56- cells with sequential sub-gates indicated above each plot. **(b)** Co-expression of CD8α and CD8β and lack of CD56 and CD16 expression on CD3+TCRαβ+tetramer+ T cells from TCR-transduced CB ATOs, indicating conventional T cell development. Data are representative of 3 independent experiments. **(c)** Enhanced total cell output and cell yield relative to starting number of HSPCs in TCR-transduced versus mock-transduced ATO at 6 or 7 weeks, generated with 7.5–18×10^3 starting CB HSPCs. Mean and SD of independent experiments are shown (mock n=3, TCR n=8, ** p=0.002). **(d)** Cytotoxic priming of ATO-derived TCR-engineered T cells by artificial antigen presenting cells (aAPCs). Cytokine production and CD107a membrane mobilization of tetramer+CD3+CD8SP T cells in response to K562 cells or K562 aAPCs that express CD80 and HLA-A*02:01 single chain trimers presenting an irrelevant ($MART1_{26\text{-}35}$) or cognate ($NY\text{-}ESO1_{156\text{-}165}$) peptide. Data are representative of three independent experiments. **(e)** Proliferation (CFSE dilution) and activation (CD25 upregulation) of ATO-derived CD3+tetramer+CD8SP T cells in response to irrelevant (MART1) or cognate (NY-ESO-1) aAPCs for 72h. Data are representative of two independent experiments. **(f)** Post-ATO expansion of CD3+TCRαβ+CD8SP T cells isolated from TCR-transduced ATOs relative to starting cell number, in response to anti-CD3/CD28 and either IL-2 or IL-7/IL-15 after 7 and 14 days. Mean and SD of technical triplicates are shown, and data are representative of three independent experiments. **(g)** Allelic exclusion of

endogenous TCR Vβ in CD3+TCRαβ+tetramer+CD8SP cells isolated from TCR-transduced (n=3) compared with non-transduced (n=5) ATOs as shown by flow cytometric analysis of Vβ family frequency. Error bars represent SD. **(h)** *In vitro* cytotoxicity of ATO-derived TCR-engineered T cells. CD8SP T cells from HLA-A*02:01/NY-ESO-$1_{157-165}$-specific TCR-transduced ATOs were activated with anti-CD3/28 +IL-2 for 36h and co-incubated with K562 cells, K562 cells transduced with HLA-A*02:01 single chain trimers presenting an irrelevant ($MART1_{26-35}$) or cognate ($NY\text{-}ESO1_{156-165}$) peptide (K562-MART-1 and K562-ESO, respectively), or the HLA-A*02:01 U266 multiple myeloma cell line which expresses NY-ESO-1 endogenously. Apoptosis was determined by flow cytometry for annexin V+ cells at 9h. Effector:Target (E:T) ratios were calculated based on percent tetramer+CD3+ T cells at the start of co-cultures. Data are representative of two independent experiments. **(i)** *In vivo* tumor control by ATO-derived TCR-engineered T cells. CD8SP T cells from TCR-transduced ATOs were activated and expanded for 14 days. 5.7×10^6 total T cells (4.5×10^6 antigen-specific T cells by tetramer staining) or PBS were injected intravenously into NSG mice subcutaneously implanted 3 days earlier with 2.5×10^5 luciferase-transduced K562-ESO tumor cells. Bioluminescence was recorded at the indicated timepoints. Mean and SD for each group is shown (PBS n=2, TCR-transduced ATO T cells n=3) (** p=0.00033, **** p=0.000066).